
This item was submitted to [Loughborough's Research Repository](#) by the author.
Items in Figshare are protected by copyright, with all rights reserved, unless otherwise indicated.

Treatment of winery wastewater by sulphate radicals: HSO₅⁻/transition metal/UV-A LEDs

PLEASE CITE THE PUBLISHED VERSION

<http://dx.doi.org/10.1016/j.cej.2016.04.135>

PUBLISHER

© Elsevier

VERSION

AM (Accepted Manuscript)

PUBLISHER STATEMENT

This work is made available according to the conditions of the Creative Commons Attribution-NonCommercial-NoDerivatives 4.0 International (CC BY-NC-ND 4.0) licence. Full details of this licence are available at: <https://creativecommons.org/licenses/by-nc-nd/4.0/>

LICENCE

CC BY-NC-ND 4.0

REPOSITORY RECORD

Rodriguez-Chueca, Jorge, Carlos Amor, Tania Silva, Dionysios D. Dionysiou, Gianluca Li Puma, Marco S. Lucas, and Jose A. Peres. 2016. "Treatment of Winery Wastewater by Sulphate Radicals: Hso₅⁻/transition Metal/uv-a Leds". figshare. <https://hdl.handle.net/2134/22973>.

Treatment of winery wastewater by sulphate radicals:

HSO₅⁻/transition metal/UV-A LEDs

Jorge RODRÍGUEZ-CHUECA¹, Carlos AMOR¹, Tânia SILVA¹, Dionysios D.

DIONYSIOU², Gianluca LI PUMA³, Marco S. LUCAS^{1,3*}, José A. PERES¹

(1) Centro de Química de Vila Real, Departamento de Química, UTAD - Universidade de Trás-os-Montes e Alto Douro, 5000-801 Vila Real, Portugal

(2) Environmental Engineering and Science Program, Department of Biomedical, Chemical and Environmental Engineering (DBCEE), 705 Engineering Research Center, University of Cincinnati, Cincinnati, OH 45221-0012, USA

(3) Environmental Nanocatalysis and Photoreaction Engineering, Department of Chemical Engineering, Loughborough University, Loughborough LE11 3TU, United Kingdom

Submitted to **Chemical Engineering Journal**

*Author to whom correspondence should be addressed:

Tel: +44 (0) 1509 222 698; Email: m.p.lucas@lboro.ac.uk

ABSTRACT

In this study, the effectiveness of the $\text{HSO}_5^-/\text{M}^{n+}/\text{UV}$ process on the treatment of winery wastewater (WW) was investigated. The optimal operating conditions were determined: $[\text{HSO}_5^-] = 2.5 \text{ mM}$; $[\text{M}_2(\text{SO}_4)_n] = 1.0 \text{ mM}$; $\text{pH} = 6.5$ and reaction temperature = 323 K . Under the given conditions, 51%, 42% and 35% of COD removal was achieved using respectively Fe(II), Co(II) and Cu(II) as catalysts. Different UV sources were tested with the previously selected optimal conditions in order to increase the treatment efficiency. The highest COD removal (82%) was achieved using a UV-A LEDs system (70 W/m^2). These conditions were also promising for the treatment of WW with COD concentrations of $5000 \text{ mg O}_2/\text{L}$, reaching 79% and 64% of COD and TOC removal, respectively, after 180 minutes of treatment. At 323 K , the most effective treatment was obtained when Co(II) was used as catalyst (79% and 64% of COD and TOC removal), while at ambient temperature (293 K) the highest COD (65%) and TOC (52%) removals were obtained with Fe(II) catalyst. Moreover, it was demonstrated that the use of $\text{HSO}_5^-/\text{M}^{n+}$ in several consecutive doses was more efficient than adding the reagents as a single dose at the beginning of the reaction. A comparison between the performance of the $\text{HSO}_5^-/\text{Fe(II)}/\text{UV-A LED}$ process and the conventional photo-Fenton demonstrated important advantages associated with the $\text{HSO}_5^-/\text{Fe(II)}/\text{UV-A LED}$ process, including the absence of the costly pH adjustment and of the hydroxide ferric sludge which characterize the photo-Fenton treatment process. The $\text{HSO}_5^-/\text{M}^{n+}/\text{UV-A LED}$ process demonstrates a high COD and TOC removal efficiency, and it can be considered a promising technology for application in real scale agro-food wastewater treatment plants.

Keywords: winery wastewater; SR-AOPs; peroxymonosulphate; UV LEDs; cobalt; iron.

1. Introduction

The agricultural food industries produce large volumes of wastewater containing high concentrations of organic materials, which are occasionally discharged into municipal wastewater systems [1-3]. These effluents are mainly originated from various unit operations such as washing, crushing and pressing of food and grapes, as well as, the rinsing of fermentation tanks, barrels and other equipment [4, 5].

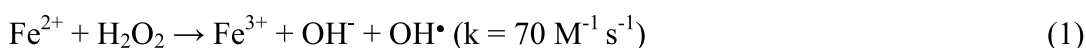
A winery typically produces around 1.3 – 1.5 kg of effluent per litre of wine produced. A high organic load of soluble sugars, organic acids, alcohols, polyphenols, tannins and structural polymers [6, 7] and an acidic pH characterize these effluents. In addition, these effluents present a seasonal variability and unpleasant odours, causing environmental and aesthetic problems in the wine producing countries.

The European Directive 91/271/EEC classifies these effluents as similar to urban wastewater [8]. For this reason, a high number of winery industries use wastewater treatments methods resembling those used in Municipal Wastewater Treatment Plants (MWWTP). However, conventional wastewater treatments do not work satisfactorily due to the seasonal variability and the high organic concentration of winery effluents. For these reasons, Advanced Oxidation Processes (AOPs) are gaining importance in the treatment of these effluents, due to the capacity of generating free radicals, which can attack and degrade the complex molecules found in winery wastewater.

AOPs can be classified on the basis of the radical species generated as hydroxyl based ($\text{HO}\cdot$; HR-AOPs) or sulphate based ($\text{SO}_4\cdot$; SR-AOPs). The most common HR-AOPs are based on the photolysis of hydrogen peroxide (UV- H_2O_2 process) or in the combination of a semiconductor photocatalyst (e.g., TiO_2 or iron oxides) with an oxidant (e.g., oxygen or hydrogen peroxide) and UV radiation; this is the case of TiO_2 -photocatalysis

and the photo-Fenton reaction. The powerful hydroxyl radical generated are able to oxidize a large variety of organic compounds [9, 10] and inactivate a wide range of microorganisms [11, 12].

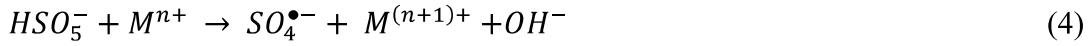
Fenton's reagents oxidation (HR-AOPs) is a homogeneous catalytic oxidation process based on the decomposition of hydrogen peroxide by ferrous ions resulting in the generation of hydroxyl radicals HO• [13-16]. The production of HO• is greatly increased by UV-vis radiation of wavelength up to 600 nm (photo-Fenton process). Photo-Fenton produces hydroxyl radicals via a series of catalytic cycle reactions with iron [Fe(II) and Fe(III)], H₂O₂ and UV radiation. The highest photo-Fenton efficiency is found at pH 2.8 [17], since iron salts precipitate far from this pH value. These reactions are summarized as follows:



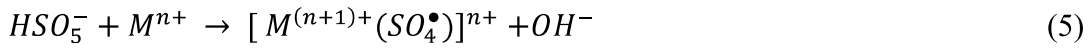
Recently, sulphate radical-based AOPs (SR-AOPs) are gradually attracting attention as *in situ* chemical oxidation technologies, complementing HR-AOPs. Sulphate radicals processes are based in the addition of chemical oxidants as persulphate salts, such as Na₂S₂O₈, K₂S₂O₈ and KHSO₅ [18].

Peroxymonosulphate (HSO₅⁻; PMS) is the active ingredient of a triple potassium salt, 2KHSO₅•KHSO₄•K₂SO₄. This salt has some advantages when compared to hydrogen peroxide. For instance, the oxidation potential of HSO₅⁻ ($E^\circ_{\text{HSO}_5^-/\text{HSO}_4^-} = 1.82 \text{ V}$) is higher than hydrogen peroxide ($E^\circ_{\text{H}_2\text{O}_2/\text{H}_2\text{O}} = 1.78 \text{ V}$), although lower than hydroxyl radical ($E^\circ_{\text{HO}\cdot} = 2.80 \text{ V}$). Moreover, PMS is relatively stable at ambient temperature and easy to handle since it is in a powder form. However, PMS presents some disadvantages such as that it reacts slowly with organic species at ambient temperature.

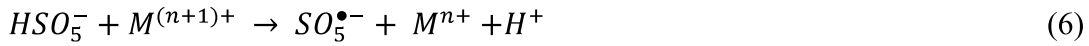
PMS can be easily activated into highly reactive radicals by two different routes: i) through homolytic cleavage of the peroxide bond of HSO_5^- by photolysis or thermolysis (Eq. 3); ii) via one electron transfer by transition metal (Eq. 4 – 6) [19-21].



M = Co(II), Fe(II) and Ru(III)



M = Ce(III), Mn(II), Ni(II)



M = Ce(IV), Fe(III), Mn(III)

The efficient activation of HSO_5^- through the use of different transition metals such as Fe(II), Co(II) Ni(II), and other metals, has been reported in literature [20, 22]. However, it is not clear which transition metal is the most effective for the activation of HSO_5^- . For instance, the coupling of $\text{HSO}_5^-/\text{Fe(II)}$ is one of the most common combination, but it presents some disadvantages similar to the Fenton reaction, such as a slow regeneration of Fe(II) from Fe(III) and the production of a ferric hydroxide sludge [20]. In contrast, the coupling of $\text{HSO}_5^-/\text{Co(II)}$ presents some advantages in comparison with Fenton reaction, including the possibility of applying the $\text{HSO}_5^-/\text{Co(II)}$ process without pH adjustment [23, 24].

Within this background, the main objective of this study was to evaluate the performance of SR-AOPs ($\text{HSO}_5^-/\text{M}^{n+}/\text{UV}$) as a new and emerging process for the treatment of winery wastewater. In this study we determined the most effective

operational conditions of the $\text{HSO}_5^-/\text{M}^{n+}/\text{UV}$ oxidation process such as pH, temperature, dosage of HSO_5^- , the impact of transition metal salts ($\text{M}_2(\text{SO}_4)_n$) and the influence of different artificial UV radiation sources. Finally, the $\text{HSO}_5^-/\text{M}^{n+}/\text{UV}$ oxidation process performance was compared with the photo-Fenton treatment of winery wastewater performed under the same operational conditions, to determine the benefits of this new treatment process.

2. Materials and Methods

2.1. Winery wastewater

Four different winery wastewater effluents were sourced. The pH of these effluents was in the range 3.6 to 4.0 and the COD load ranged from 513 to 5391 mg O_2/L . Table 1 summarizes the physico-chemical characteristics of the winery effluents.

Table 1

2.2. Reagents

The SR-AOPs were carried out with different dosages of potassium peroxymonosulphate (PMS; $2\text{KHSO}_5 \cdot \text{KHSO}_4 \cdot \text{K}_2\text{SO}_4$; Merck) coupled with different concentrations of transition metals ($\text{CoSO}_4 \cdot 7\text{H}_2\text{O}$; ZnSO_4 ; NiSO_4 ; CuSO_4 ; $\text{FeSO}_4 \cdot 7\text{H}_2\text{O}$; Ag_2SO_4 ; MgSO_4 or MnSO_4 ; Panreac). Sulphuric acid (H_2SO_4 ; Scharlau) and sodium hydroxide (NaOH ; Panreac) were used for pH adjustment. H_2O_2 (30% w/w, Scharlab) was used to carry out the Fenton and photo-Fenton treatments. All the reagents used were analytical grade.

2.3. Analytical determinations

Different physico-chemical parameters such as pH, conductivity, redox potential, turbidity, Total Suspended Solids (TSS), Chemical Oxygen Demand (COD), Total Organic Carbon (TOC) and Total Polyphenols (TP) were analyzed for the samples characterization. In addition, values of COD and TOC were analyzed during the treatments in order to assess the efficiency of the treatments.

Chemical Oxygen Demand was measured according to 410.4 Method of Environmental Protection Agency of USA [25], using a HACH DR/2400 portable spectrophotometer. Total Carbon (TC) and Total Inorganic Carbon (TIC) were separately determined by catalytic combustion at 680°C (Standard Methods 5310B [26]) and acidification, respectively, both using a non-dispersive infrared detector (NDIR) in a TOC-L CSH/CSN analyzer equipped with an ASI-L autosampler (Shimadzu). Total organic carbon (TOC) was given by the difference between TC and TIC. The pH and redox potential were determined by a HANNA pH 209 laboratory meter following the Standard Method 4500-H⁺-B and 2580, respectively [26], while conductivity was measured by a Crison Basic as indicated in ISO 7888:1985 [27]. Turbidity was measured according ISO 7027:1999 [28] using a HACH 2100 IS Turbidimeter, while Total Suspended Solids (TSS) were measured by spectrophotometry according to Standard Method 2540D using a HACH DR/2400 portable spectrophotometer [26]. Finally, the concentration of Total Polyphenols (TP), (mg gallic acid/L), was determined by spectrophotometry using the Folin-Ciocalteu reagent (Merck) [29]. UV-vis measurements were carried out using a Jasco V-530 UV/VIS spectrophotometer.

2.4. UV radiation sources

Three UV radiation sources were used: i) a *Heraeus* TNN 15/32 low pressure mercury vapour lamp and ii) two UV-A LEDs systems.

Heraeus TNN 15/32 mercury lamp

Batch experiments were performed in a *Heraeus* photoreactor (height 18 cm; diameter 8 cm). The cylindrical reactor of 800 mL capacity was made of borosilicate glass with ports, in the upper section, for sampling. The photoreactor was fitted with a *Heraeus TNN 15/32* lamp (14.5 cm in length and 2.5 cm in diameter) mounted in the axial position inside the reactor. The spectral output of the low-pressure mercury vapour lamp emits mainly (85–90%) at 253.7 nm and about 7–10% at 184.9 nm. The reaction temperature in the reactor was kept at the desired value within ± 0.5 °C by using a thermostatically controlled outer water jacket. The reactor was loaded with 500 mL of winery wastewater and continuous mixing was maintained by means of a magnetic stirrer.

UV-A LEDs radiation (365 and 370 nm)

The photo-assisted PMS/metal reactions were carried out in a lab-scale batch reactor which was illuminated with two different UV-A LED photo-systems [30, 31]. The applied UV radiation in the first photo-system was generated by a matrix of 96 Indium Gallium Nitride (InGaN) LEDs lamps (Roithner RLS-UV370E) which illuminated an area of 11 x 7 cm². These LEDs have a light peak emission at 370 nm, and the nominal consumption of each LED lamp was 80 mW when the applied current was 20 mA. The maximum average optical power was, approximately, 100 mW. The array optical emission was controlled with a pulse width modulation (PWM) circuit that modulated the electric current supplied to each LED in the array. The current supplied had a square waveform with two states: 0 mA (LED emission OFF) and 30 mA (LED emission ON) and a frequency of 350 Hz. The PWM module allowed the configuration of the ON

state time duration in each cycle between 0 and 100% of the cycle period and, consequently, the emitted average optical power was modulated between 0 and 100 mW depending on value of the root mean square (RMS) of the electric current intensity waveform supplied to the LED array by the PWM module. The system irradiance was measured using an UV enhanced Si-photodetector (ThorLabs PDA155) in a configuration that replicates the one used in the photoreactor. In this system, the output optical power was controlled using a pulse width modulation (PWM) circuit and the RMS current intensity was measured with a multimeter (UniVolt DT-64).

The second and more powerful photo-system consisted by a matrix of 12 InGaN LEDs lamps (Roithner APG2C1-365E LEDS) with a maximum emission wavelength at 365 nm. The nominal consumption of each LED lamp was 1.4 W at an applied current of 350 mA. The output optical power was controlled by maintaining the forward current constant using a power MOSFET with six different allowed current settings.

The photoirradiation treatments were carried out with a RMS current intensity of 240 mA in the first UV-A LED photo-system, corresponding to a UV irradiance of 23 W/m² and a photon flux of 5.53×10^{-7} Einstein/s. The second photo-system irradiance was 70 W/m² and the corresponding photon flux was 1.64×10^{-6} Einstein/s.

2.5. Electrical energy determination

The figure-of-merit electric energy per order (E_{EO}) [32] was used to evaluate the efficiency of the AOP used. This parameter refers to the electric energy in kilowatt hours (kWh) required to reduce the concentration of a pollutant C by one order of magnitude in a unit volume (1000 L) of contaminated water. E_{EO} can be calculated as follows (Equation 7):

$$E_{EO} = \frac{P \cdot t \cdot 1000}{V \cdot \log\left(\frac{C_i}{C_f}\right)} \quad \text{Batch mode} \quad (7)$$

Where P is the rated power (kW) of the system, V is the volume (L) of water treated in time t (h), C_i and C_f are the initial and final concentrations, and the factor of 1000 converts g to kg. Higher E_{EO} values correspond to lower removal efficiencies.

2.6. Experimental procedure

All the experiments were carried out in duplicate and values presented are the average of both results. The observed standard deviation was always less than 5% of the reported value.

PMS treatments (SR-AOPs)

Batch experiments were performed on 500 mL of winery wastewater. The pH of the winery wastewater was initially adjusted using H_2SO_4 or NaOH and measured by a 209 pH meter from Hanna Instruments. Then, the effluent was heated to the operating temperature, which was in the range from 293 to 323 K. Finally, the assay started when the dosage of PMS (1 – 20 mM) and the metal sulphate catalyst (0.1 – 8 mM) were added to the effluent at the same time. In the photo-assisted experiments the assay started when the UV radiation system was switched on, also corresponding to the addition of PMS and catalyst. During the course of the reaction samples were withdrawn at periodic interval and analysed.

Fenton and photo-Fenton treatments (HR-AOPs)

Batch experiments were performed on 500 mL of winery wastewater. The second UV-A LED system was used in the photo-Fenton experiments. The pH of the winery

wastewater was initially adjusted to 3 or 6.5, using H_2SO_4 or NaOH . Then, the effluent was heated to the operating temperature, which was in the range from 293 to 323 K, and subsequently $\text{FeSO}_4 \cdot 7\text{H}_2\text{O}$ (1 – 8 mM) was added to the effluent. Finally, hydrogen peroxide (range 2.5 to 20 mM) was directly added to the photoreactor at the beginning of each experiment. Samples of the treated effluent were withdrawn during the course of the reaction, at predetermined time intervals and analysed. The concentration of H_2O_2 was monitored via Merckoquant peroxide analytical test strips (Test Peroxides, Merck Merckoquant). Na_2SO_3 (Panreac[®]) was added to water samples to eliminate residual hydrogen peroxide in each sample. In addition, the temperature of the samples was monitored.

3. Results and discussion

3.1. SR-AOPs

Optimization of operational conditions

The role of different operating parameters such as pH, temperature, PMS concentration, type of transition metal and concentration, as well as the UV radiation source were investigated to establish the optimal operational conditions for the treatment of winery wastewater with the SR-AOPs. In these experiments, winery wastewater with a COD concentration of approximately 500 mg O_2/L was used. Initially, the pH was varied in the range 2 to 8 to determine the pH that achieved the fastest COD removal, with a PMS concentration of 4.0 mM, without metal catalyst, at 293 K and in the absence of UV radiation during the 90 minutes run. Subsequently, the same set of experiments was carried out by adding 1.6 mM of $\text{CoSO}_4 \cdot 7\text{H}_2\text{O}$ metal catalyst.

Figure 1

Figure 1A shows the COD removal obtained as a function of the initial pH. In the absence of the sulphate salt, the COD removal did not exceed 10%, while in the presence of $\text{CoSO}_4 \cdot 7\text{H}_2\text{O}$, 20% COD removal was reached. The highest removals were achieved at pH 5.0 and 6.5. The last one was chosen as optimal pH since it is nearer to neutral pH. These results are supported by those obtained by Sun et al. for the treatment of landfill leachate [33]. On the other hand, the optimal pH is a function of the chemical and physical nature of the effluent and some authors have reported acidic pH values as optimal for the removal of pharmaceuticals and dyes [34, 35]. Nevertheless, this study suggests that the PMS can also be used at neutral pH obtaining relatively high COD removals in water and urban wastewater treatment thus avoiding the pre- and post-adjustment of pH of the effluents. In the case of the winery wastewater, a slight pre-adjustment of the pH is required, because of the acidic condition of this kind of effluents.

Some authors reported the need of thermal activation of PMS [21, 36]. Figure 1B shows the COD removal as a function of temperature after 90 minutes of treatment, using the optimal pH (6.5) and 4.0 mM of PMS and 1.6 mM of $\text{CoSO}_4 \cdot 7\text{H}_2\text{O}$. The results show no differences between treatments carried out at ambient temperature (293 K) and 313 K, however, the COD removal increased significantly at temperatures above 313 K, doubling COD removal at 333 K. In further experiments, the operating temperature of 323 K was selected since higher temperatures result in an increase in the energy requirement to heat the water.

After pH and temperature optimization, several dosages of PMS were applied in the range from 0 to 20 mM. Figure 1C shows the results after 90 minutes of treatment carried out at pH 6.5 and 323 K. A sharp increase in COD removal was observed up to

2.5 mM, followed by a plateau from 2.5 – 7.0 mM, with a COD removal around 42% and to a further increase in the COD removal at higher PMS dosages, such as 10 and 20 mM reporting 50% and 68% of COD removal, respectively. Taking into account economic factors related to the cost of reagents, 2.5 mM was chosen as an optimal PMS dosage.

Finally, the optimization of the concentration of $\text{CoSO}_4 \cdot 7\text{H}_2\text{O}$ in the range 0 to 5 mM was carried out using the optimal conditions obtained previously. The COD removal after 90 minutes of treatment reached a maxima (Figure 1D) at 1 mM of $\text{CoSO}_4 \cdot 7\text{H}_2\text{O}$. Thus the optimal ratio PMS:Co(II) was 2.5:1, which obtained 43% of COD removal after 90 minutes of treatment. Sun et al. also observed a reduction of the COD removal at high Co(II) dosages [33]. They reported an optimal ratio PMS:Co(II) of 10^4 , therefore being 4.5 mM and $4.5 \cdot 10^{-4}$ the suitable dosages of PMS and Co(II), respectively, to mediate PMS decomposition in the treatment of landfill leachate (COD = 1116 mg/L). Wang and Chu observed that an excessive ferrous ion concentration will retard the process due to the $\text{SO}_4^{\bullet-}$ scavenging effect by an excess of Fe(II) [21]. In the case of using Co(II), a similar behaviour could be considered.

In further experiments, the effect of the metal species in the sulphate catalysts (ZnSO_4 , NiSO_4 , CuSO_4 , CoSO_4 , FeSO_4 , Ag_2SO_4 , MgSO_4 and MnSO_4) which is responsible for the activation of HSO_5^- , was investigated. These sulphate salts were tested in experiments lasting 90 min, carried out at pH 6.5, 323 K and using a PMS dosage of 2.5 mM over winery effluents with a COD concentration of 500 mO_2/L . Higher COD removals (Figure 2) were obtained with CuSO_4 , CoSO_4 and FeSO_4 , reaching 35, 43 and 51%, respectively. Co(II) has been reported as the most effective metal catalyst for the activation of HSO_5^- , which further promotes a radical sulphate cascade mechanism [33,

37, 38]. Anipsitakis and Dionysiou [19, 22, 39] investigated different transition metals as catalysts for the decomposition of PMS. The reduction of Co(III) to Co(II) mediated by the oxidation of PMS is thermodynamically feasible (0.82 V) and fast, and the process proceeds cyclically many times until PMS is totally consumed [22]. However, in this reaction the Co(II) product formed is toxic and represents a serious risk to the environment if discharged with the effluent. Therefore, in this study Fe(II) sulphate was investigated for the treatment of winery wastewater as a replacement for Co(II), especially since the combination PMS/Fe(II) achieved COD removals of the same order as those obtained with Co(II). The main advantage of using Fe(II) as PMS activator lies in the synergistic effect with UV radiation, which produces sulphate and hydroxyl radicals, both of which enhance the degradation of organic matter in the winery wastewater. In this case, the catalytic cycle Fe(III)/Fe(II) is accelerated by the photo-reduction of Fe(III)-complexes. Regarding the solution pH, Fe(III) can exist as ferric ions and/or Fe(III)-complexes which in some cases act as photosensitizers, such as $\text{Fe}(\text{OH})^{2+}$ according to Eq. 2 [21, 37-42]. Besides, significant results of COD removal were achieved with the combination of PMS/Cu(II). Ji et al. described the activation of PMS through combination with CuO, demonstrating the efficiency of this catalyst [43], and Madhavan et al. compared the coupled system Cu(II)/PMS and Fe(III)/PMS assisted by visible light [44].

Figure 2

As observed, PMS can be activated through a high number of variables; nevertheless, other authors do not report the use of all of these activation agents. Besides, the operational conditions can vary with the chemical composition of each effluent. Sun et al. achieved optimal conditions to treat landfill leachate through the combination of

PMS/Co(II)/heating [33]. These optimal conditions present certain similarities with those obtained in this work. Sun et al. established as optimal pH 6.5, dosages of PMS and Co(II) of 4.5 mM and 4.5×10^{-4} mM, respectively, and temperature of 303 K [33]. Under these conditions, a COD removal of 57.5% was achieved after 300 minutes of treatment. This COD removal is significantly lower than the removals reported in this paper, using a lower dosage of PMS and during approximately half of the time.

PMS/Mⁿ⁺/UV radiation

In order to increase the rate of organic matter removal, different UV radiation sources, including low pressure UV mercury lamp and UV-A LEDs lamps, were applied in combination with the optimal experimental conditions obtained in section 3.1. (2.5 mM PMS; 1 mM $\text{CoSO}_4 \cdot 7\text{H}_2\text{O}$; pH = 6.5; T = 323 K). Figure 3 shows that most of the COD removal was obtained during the first 20 minutes of treatment. The highest values were achieved using the UV-A LEDs lamps with an irradiance of 70 W/m^2 (80%), followed by the UV-A LEDs lamps with 23 W/m^2 (62%) and the low pressure UV mercury lamp (55%) after a reaction time of 120 minutes, suggesting that the reaction is initially photon limited. As expected, the experiments performed without UV radiation reached a plateau at much lower COD removals (24%) due to the lack of sulphate radicals, after that Co(II) was totally consumed. A similar saturation kinetics was observed in the photo-assisted treatments, but the plateau is approached at much higher COD removals and much longer reaction times. Table 2 reports the values of the Electrical Energy per Order (E_{EO}) for the different photo-assisted treatments. The low pressure mercury TNN 15/32 lamp returned a very large E_{EO} ($173 \text{ kWh/m}^3/\text{order}$) in consequence of the high electrical consumption of these types of UV lamp. In contrast, the UV-A LED photo-systems (162 and $98 \text{ kWh/m}^3/\text{order}$) more efficient than the TNN 15/32 lamp since most of the electrical energy applied is converted to UV radiation.

Table 2

The activation of PMS by UV radiation has been reported in the literature [21, 42, 45-48]. The photolysis of PMS with visible light (419 nm) or near-UV radiation (350 nm) is negligible, however, at 254 nm becomes significant, as reported for the degradation of 2,4,5- trichlorophenoxyacetic acid [21]. The photolysis of PMS, produces one mole of sulphate radical and one mole of hydroxyl radical per each mole of peroxymonosulphate (reaction 3). Thus, if the wavelength is higher than 260 nm, little or no photochemical decomposition of PMS was observed. However, the treatment of winery wastewater by the combination of PMS/Mⁿ⁺/UV radiation, did not show significant differences when the radiation wavelength was varied, and significant COD removal was achieved with UV-A LED radiation.

The treatment of winery wastewater by the PMS/Mⁿ⁺/UV process was performed at different COD concentrations (500, 900, 1900 and 5000 mg O₂/L) to investigate the treatment efficiency in more concentrated effluents which are more difficult to treat. Table 3 shows the COD reduction after the application of the most effective operating conditions (2.5 mM PMS; 1 mM CoSO₄·7H₂O; pH = 6.5; T = 323 K; UV-A LEDs 70 W/m²).

Table 3

From Table 3, the COD removal it is almost the same independently of the initial COD concentration. Therefore, after 180 minutes, 3950 mg O₂/L of COD were removed from an initial concentration of 5000 mg O₂/L. However, the COD removal rate (mg COD removed/min) increases accordingly with the concentration of organic matter. When

treatments were applied over effluents with a COD load of 500 mg O₂/L a removal rate 2.22 mg/min was obtained. Meanwhile, over more concentrated effluents, e.g. 5000 mg O₂/L, a removal rate of 19.33 mg/min was observed. Thus, a higher amount of COD was removed per minute when the effluent presents a higher organic load. Further experiments were carried out using the effluent with the highest COD load, because such treatment process was able to remove a higher amount of organic matter with the same operating conditions. However, a pre-treatment step can be applied to reduce the COD load and consumption of reagents and energy during the photocatalytic PMS/Mⁿ⁺/UV process.

Application of most effective operational conditions

Different treatments were carried out in order to assess the influence of Co(II) and Fe(II) in combination with PMS, as well as, the influence of temperature when this was above ambient temperature, and the influence of an increase of PMS and transition metal concentration, keeping the molar ratio of PMS:Mⁿ⁺ constant. Figure 4A shows the results of COD and TOC reduction in treatments carried out at 323 K, while Figure 4B shows the results obtained at ambient temperature. As it can be observed in Figure 4A, the experiments performed with Co(II) achieved slightly higher COD removal rate than those performed with Fe(II), but the plateau values achieved are approximately the same, suggesting the consumption of the limiting reactant [Mⁿ⁺ = Fe(II) or Co(II)]. Moreover, it was observed that an increase in the concentrations of PMS and transition metal, at constant PMS:Metal molar ratio (2.5:1), resulted in a decrease in the final COD removal which was also observed in the TOC results. In terms of TOC removal, there was no difference in the removal rates observed with both metals. In all the treatments at 323 K it was observed that both the rates of removal of COD and TOC

decreased after 90 minutes. The rate decrease might be a direct consequence of the decrease of concentration of reactant species in solution.

Figure 4

On the other hand, the behaviour was opposite when the treatment was carried out at ambient temperature. Figure 4B shows that the COD and TOC removals were considerably lower at ambient temperature than at 323 K. However, the most important difference lies in that the higher COD removals were obtained through the combination of PMS with Fe(II) and using the highest concentrations PMS:Fe(II) (20:8 mM). During the first 60 minutes of treatment, the COD removal with Fe(II) catalyst was 48% and with Co(II) catalyst was 34% at the same molar ratio. After 180 min of the treatment the COD removals were 65 and 56% with Fe(II) (0.0057 min^{-1}) and Co(II) (0.0039 min^{-1}) respectively. At lower concentration and same molar ratio (2.5:1 mM; PMS:Metal) the COD removal proceeded at slower rates although the final COD removals after 180 min were similar to those obtained with the highest dosage of reagents, 64 and 52% with Fe(II) (0.0051 min^{-1}) and Co(II) (0.0038 min^{-1}), respectively. The TOC removals observed, which ranged from 50 to 60% (Figure 4B), also agree with the general trend observed on the removal of COD.

The removal of total polyphenols (TP) through the application of PMS/Mⁿ⁺/UV-A LED process at ambient temperature and 323 K is shown in Table 4 (TP removal results after 180 minutes of treatment). The highest TP removal was obtained at conditions of ambient temperature combining 2.5 mM of PMS and 1 mM of Co(II) reaching a value of 70%, which are different than the conditions that obtained the highest COD and TOC removal. A similar TP removal, 69%, was obtained but combining 8 mM of Fe(II) with 20 mM of PMS. The TP removal decreased with the increase of temperature until 323

K, reaching maximum removals of 56 and 55% using 8 mM of Co(II) and Fe(II), respectively, with 20 mM of PMS.

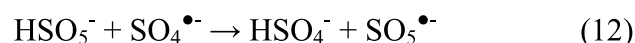
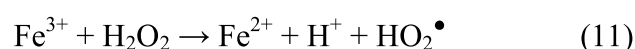
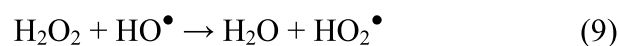
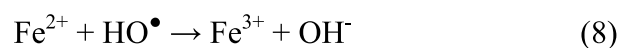
Table 4

Finally, the effect of the dosing procedure of the reagents was investigated using one dose or multiple dosing steps of PMS and $\text{CoSO}_4 \cdot 7\text{H}_2\text{O}$. A higher dosage of PMS and $\text{CoSO}_4 \cdot 7\text{H}_2\text{O}$ (20 and 8 mM) using the same molar ratio (2.5:1) was selected and the solution was irradiated with UV-A LED radiation (70 W/m^2) at pH 6.5 and 323 K. In the first set of experiments, the total amounts of PMS and Co(II) were added as a single dose at the beginning of the assay. Whilst, in the other set of the experiments, these reagents were added in six different dosing stages, every 30 minutes, so that in the last addition the total concentrations of PMS and Co(II) added to the solution were 20 and 8 mM, respectively. The results presented in Figure 5 show no significant differences during the first 15 minutes of treatment, however thereafter, the COD removal increased when the reagents were added in stages. The final COD values after 180 min of treatment were 86% using multiple dosing and 70% using a single dose. In the absence of UV-A LED radiation a similar behaviour was observed, but at a reduced rate. In this case, the addition of reagents as a single dose, removed COD faster during the first 60 minutes of treatment, due to the faster generation of radical species at higher concentration of reagents.

Figure 5

The above behaviour can be understood by considering the scavenging reaction of hydroxyl (reactions 8-11; [49]) and sulphate radicals (reaction 12; [50]). At the

beginning of the reaction the production of radicals is very rapid since the concentration of reagents is very high and the oxidation process is dominated by the production of radicals.



This results in a fast oxidation of the organic matter, however, in parallel the scavenging reactions also proceed at fast rate and the final COD removal does not reach its maximum value. In contrast, the addition of reagents in multiple doses keeps their concentration low in the reactor suppressing the rate of the scavenging reactions, and as a result a more gradual supply of radical species results in a significantly higher final COD removal (82%). This value approaches the same COD removal obtained at higher temperature (323 K) with a single dose of reagents, suggesting that it could be possible to reduce the operating costs, performing the treatment at ambient temperature and with a staged addition of reagents. The influence of number of dosing steps has also been reported by other authors both for the Fenton and the PMS/Co(II) oxidation. Deng and Englehard studied the behaviour in the treatment of landfill leachate by Fenton process, and considered that a single-step addition of the reagents may cause self-decomposition of oxidants due to high concentrations at the point of injection [51]. Sun et al. also tested various numbers of stepwise additions in the treatment of landfill leachate using

Fenton and PMS/Co(II) oxidation processes [33] and reported that three and seven doses resulted in a faster treatment of the leachate.

3.2. HR-AOPs. Photo-Fenton treatments

The efficiency of SR-AOPs in the treatment of winery wastewater was benchmarked against the photo-Fenton reaction process, which was applied using the same operational conditions in terms of pH, temperature, Fe(II) concentration and oxidant concentration, in this case H₂O₂. Figure 6 shows the COD and TOC removal at pH 6.5 at 323 K (Figure 6A) and at ambient temperature (Figure 6B) comparing the treatment of winery wastewater with the SR-AOP and photo-Fenton processes.

Figure 6

The photo-Fenton assays carried out at pH 6.5 using 2.5/1 mM H₂O₂/Fe(II) (Figure 6A) achieved the highest COD removal (85%) and faster removal rate. The COD removal with photo-Fenton was slightly higher than that obtained with the same concentrations of PMS/Fe(II)/UV (79%), despite the photo-Fenton treatment was performed at neutral pH, which differs from the optimum conditions at acidic pH. In addition, at the higher reagents dose, at the same molar ratio, the COD removals decreased to 72 and 63% with the photo-Fenton reaction and PMS/Fe(II)/UV-A LED process. Although the rate of production of radical species may be considered the same at higher and lower dosages, since the molar ratio of the reagents remained unchanged, the scavenging effect of H₂O₂ on the hydroxyl radicals generated, may contribute to the decrease in COD removal. A similar behaviour has been observed with sulphate radicals when PMS was in excess in

the reaction system [33]. Besides, an excess of Fe(II) would also contribute to the scavenging of $\text{SO}_4^{\bullet-}$ radicals [21, 50], as can be observed in the equation 13 [52]:



In terms of TOC removal, the highest mineralization of organic matter was obtained through the treatment 20:8 mM H_2O_2 :Fe(II) in photo-Fenton treatments with a value of 74%, while at the same conditions the treatment PMS/Fe(II)/UV-A LED achieved 56%. On the other hand, the yields were similar in both treatments when the used concentrations were 2.5:1 mM oxidant:Fe(II), reaching 66% with PMS and 65% with H_2O_2 . In conclusion, contaminant removal by the photo-Fenton process proceeded at faster rates than PMS/Fe(II)/UV-A LED treatments. However, it is necessary to take into account some aspects to distinguish both treatments, making difficult their comparison. Firstly, in the case of photo-Fenton assays, it was required to perform new additions of hydrogen peroxide when the concentration of this oxidant agent decreased to very low values in order to continue with the photo-Fenton process. Therefore, in those treatments carried out with 2.5 mM of H_2O_2 a total amount of 10 mM hydrogen peroxide was consumed, while in the treatments with 20 mM of H_2O_2 a final total amount of 100 mM was consumed, so 4 and 5 H_2O_2 doses were required respectively. These supplementary doses of oxidant reagent were not necessary in the PMS/Fe(II)/UV-A LED treatment process.

Figure 6B shows the results obtained after the application of the same processes but at ambient temperature (293 K). The treatments with PMS were faster than photo-Fenton process both in COD and TOC removal. The final COD and TOC removal after 180 minutes, were similar with values around 65% and 53%. In both cases the highest removal rate corresponded with the treatment 20 mM PMS and 8 mM of Fe(II). Again,

in the photo-Fenton reactions it was necessary to carry out further doses (2 and 3, respectively) of H_2O_2 when each one was consumed, reaching a total concentration of 5 and 60 mM in the treatments with 2.5 and 20 mM of hydrogen peroxide, respectively. Finally, one of the most important disadvantages of the photo-Fenton is the generation of sludge. For instance, in the treatments with 20 mM of H_2O_2 and 8 mM of Fe(II), values of 600 mg/L and 717 NTU of total suspended solids and turbidity, respectively, were observed at the end of the treatment. This situation was less significant in the experiments carried out with PMS/Fe(II) process, with values lower than 50 mg/L and 120 NTU for TSS and turbidity, respectively.

The above experiments were all carried out at near neutral pH of 6.5. However, the application of the photo-Fenton processes at pH 3, at both ambient temperature and 323 K yielded high COD removals (Figure 7) up to 89% at 323 K with the highest dosages of reagents (20/8 mM $\text{H}_2\text{O}_2/\text{FeSO}_4 \cdot 7\text{H}_2\text{O}$) and 70% at ambient temperature. Moreover, using eight times lower reactant concentrations (2.5:1 mM $\text{H}_2\text{O}_2:\text{FeSO}_4 \cdot 7\text{H}_2\text{O}$), the difference in the COD removal was only 19% and 27% lower at 323 and 293 K, respectively.

Figure 7

In summary, the application of the $\text{HSO}_5^-/\text{M}^{n+}/\text{UV-A}$ LED process presents some important advantages. First, $\text{SO}_4^{\bullet-}$ possesses an oxidation potential (2.5–3.1 V) similar or even higher than $\bullet\text{OH}$ depending on pH conditions [53]. In addition, the use of potassium peroxymonosulphate, as a good source of the oxidant PMS (HSO_5^-), can be carried out without pre- and post-adjustment of pH previous to discharge of the treated effluents. Second, the combination of PMS with a transition metal does not generate

ferric hydroxide sludge as in the case of Fenton's reagent, however it is necessary to take into account the residual metal concentration left in the treated effluent, as well as the accumulation of sulphates in the aqueous solution. Third, the activation of PMS through the combination of a transition metal, heating or UV-A radiation, results in high rates of contaminant degradation during the first few minutes of treatment. Finally, PMS is much easier to store and handle in comparison to hydrogen peroxide. PMS/Mⁿ⁺/UV-A LED treatments could be a meaningful alternative for the treatment of winery wastewater, as a stand-alone process or as a pre- or post-treatment process in combination with a biological system. In the latter case a biodegradation study should be recommended.

4. Conclusions

This study has focused on the degradation of the organic matter from a winery wastewater through the combined use of PMS/Mⁿ⁺/UV. The optimization of the operational conditions such as pH, temperature, PMS and transition metal concentrations was investigated. Initially, different transition metals were studied in order to determine the most effective conditions for the PMS/Mⁿ⁺/UV process. From the results of this study, the following order of treatment efficiency was obtained for the PMS/Mⁿ⁺/UV ($\lambda=365$ nm) technologies: PMS/Fe(II)/UV > PMS/Co(II)/UV > PMS/Cu(II)/UV > PMS/Mg(II)/UV > PMS/Zn(II)/UV > PMS/Ni(II)/UV > PMS/Ag(I)/UV > PMS/Mn(II)/UV. Moreover, different UV sources were evaluated in terms of E_{EO} values, resulting in clear advantages in using UV-A LED photo-systems rather than systems utilizing UV low pressure mercury lamps. These results were achieved considering the global power consumption (kW) of each UV source. To sum up, the optimal conditions were: pH = 6.5; temperature = 323 K; [PMS] = 2.5 mM; [Mⁿ⁺] = 1 mM (where Mⁿ⁺ = Fe(II) or Co(II)) and UV-A LED radiation (365 nm; 70

W/m²) which achieved a COD and TOC removal of 75% and 56%, after 90 minutes in effluents with 5000 mg O₂/L of COD. UV-A LED radiation sources also are ecofriendly, have a low operational cost, and exhibit a high energy efficiency in comparison to conventional mercury lamps. When PMS/Mⁿ⁺/UV treatments were carried out at 323 K, higher COD and TOC removals were obtained through the catalysed decomposition of PMS with Co(II) (79 and 64% respectively) compared to PMS with Fe(II) (74 and 66% respectively) after 180 minutes using 2.5/1 mM PMS/Mⁿ⁺. However, the behaviour was the opposite at ambient temperature, reaching a 64 and 57% of COD and TOC removal with Fe(II) and 52% of COD and TOC removal with Co(II). This behaviour can be explained by the higher activation energy of the Co(II)/PMS system (34.3 kJ/M) comparatively to the Fe/PMS and also due to the higher photosensitivity of the Fe species in water as compared to those of Co.

Photo-Fenton treatments at pH 6.5 achieved higher COD removal than PMS/Mⁿ⁺/UV treatments at 323 K due to the high influence of heating and UV-A radiation absorption. Nevertheless, the behaviour was the opposite at ambient temperature both at pH 6.5 and pH 3.

The combined treatment PMS/Mⁿ⁺/UV-A LED presents some advantages over the photo-Fenton treatment, such as the application at neutral pH avoiding the pre- and post-adjustment of pH and no generation of ferric hydroxide sludge.

Acknowledgments

The authors are grateful to Project INNOFOOD - INNOvation in the FOOD sector through the valorization of food and agro-food by-products - NORTE-07-0124-FEDER-0000029, Project INTERACT – Integrative Research in Environment, Agro-Chains and Technology - NORTE-01-0145-FEDER-000017 and Project INNOVINE & WINE - Innovation Platform of Vine and Wine - NORTE-01-0145-FEDER-000038. Marco S. Lucas acknowledges also the funding provided by the European Union's Horizon 2020 research and innovation programme under the Marie Skłodowska-Curie grant agreement No 660969.

References

- [1] C. Amor, M.S. Lucas, A.J. Pirra, J.A. Peres. Treatment of concentrated fruit juice wastewater by the combination of biological and chemical processes. *J. Environ. Sci. Health, Part A* 47 (2012) 1809-1817.
- [2] A. Durán, J.M. Monteagudo, A. Carnicer. Photo-Fenton mineralization of synthetic apple-juice wastewater. *Chem. Eng. J.* 168 (2011) 102-107.
- [3] E.E. Ozbas, N. Tufekci, G. Yilmaz, S. Ovez. Aerobic and anaerobic treatment of fruit juice industry effluents. *J. Sci. Ind. Res.* 65 (2006) 830-837.
- [4] M.S. Lucas, M. Mouta, A. Pirra, J.A. Peres. Winery wastewater treatment by a combined process: long term aerated storage and Fenton's reagent. *Wat. Sci. Technol.* 60 (2009) 1089-1095.

- [5] R. Mosteo, M.P. Ormad, E. Mozas, J. Sarasa, J.L. Ovelleiro. Factorial experimental design of winery wastewaters treatment by heterogeneous photo-Fenton process. *Water Res.* 40 (2006) 1561-1568.
- [6] M.S. Lucas, J.A. Peres, G. Li Puma. Treatment of winery wastewater by ozone-based advanced oxidation processes (O_3 , O_3/UV and $O_3/UV/H_2O_2$) in a pilot-scale bubble column reactor and process economics. *Sep. Purif. Technol.* 72 (2010) 235-241.
- [7] L. Malandra, G. Wolfaardt, A. Zietsman, M. Viljoen-Bloom. Microbiology of a biological contactor for winery wastewater treatment. *Water Res.* 37 (2003) 4125-4134.
- [8] European Directive 91/271/EEC (1991). Official Bulletin of Europe Union L135, 30th May 1991.
- [9] C. Pablos, J. Marugán, R. van Grieken, E. Serrano. Emerging micropollutant oxidation during disinfection processes using UV-C, UV-C/ H_2O_2 , UV-A/ TiO_2 and UV-A/ TiO_2/H_2O_2 . *Water Res.* 47 (2013) 1237-1245.
- [10] S. Miralles-Cuevas, F. Audino, I. Oller, R. Sánchez-Moreno, J.A. Sánchez Pérez, S. Malato. Pharmaceuticals removal from natural water by nanofiltration combined with advanced tertiary treatments (solar photo-Fenton, photo-Fenton-like Fe(III)–EDDS complex and ozonation). *Sep. Purif. Technol.* 122 (2014) 515-522.
- [11] M.I. Polo-López, I. García-Fernández, T. Velegraki, A. Katsoni, I. Oller, D. Mantzavinos, P. Fernández-Ibáñez. Mild solar photo-Fenton: An effective tool for the removal of *Fusarium* from simulated municipal effluents. *Appl. Catal. B Environ.* 111-112 (2012) 545-554.

- [12] J. Rodríguez-Chueca, M.I. Polo-López, R. Mosteo, M.P. Ormad, P. Fernández-Ibáñez. Disinfection of real and simulated urban wastewater effluents using a mild solar photo-Fenton. *Appl. Catal. B Environ.* 150–151 (2014) 619-629.
- [13] W.G. Kuo. Decolorizing dye wastewater with Fenton's reagent. *Water Res.* 26 (7) (1992) 881-886.
- [14] J.A.S. Peres, L.H.M. Carvalho, R.A.R. Boaventura, C.A.V. Costa. Characteristics of p-hydroxybenzoic acid oxidation using Fenton's reagent. *J. Environ. Sci. Health Part A* 39 (2004) 2897-2913.
- [15] C. Walling. Intermediates in the reactions of Fenton type reagents. *Acc. Chem. Res.* 31 (1998) 155–157.
- [16] R. Chen, J. Pignatello. Role of quinone intermediates as electron shuttles in Fenton and photoassisted Fenton oxidations of aromatic compounds. *Environ. Sci. Technol.* 31 (1997) 2399-2406.
- [17] J.J. Pignatello, E. Oliveros, A. MacKay. Advanced oxidation processes for organic contaminant destruction based on the Fenton reaction and related chemistry. *Crit. Rev. Environ. Sci. Technol.* 36 (2006) 1-84.
- [18] G. Wei, X. Liang, Z. He, Y. Liao, Z. Xie, P. Liu, S. Ji, H. He, D. Li, J. Zhang. Heterogeneous activation of Oxone by substituted magnetites $Fe_{3-x}M_xO_4$ (Cr, Mn, Co, Ni) for degradation of Acid Orange II at neutral pH. *J. Mol. Catal. A Chem.* 398 (2015) 86-94.
- [19] G.P. Anipsitakis, D.D. Dionysiou. Radical generation by the interaction of transition metals with common oxidants. *Environ. Sci. Technol.* 38 (2004) 3705-3712.

- [20] Z.H. Wang, R.X. Yuan, Y.G. Guo, L. Xu, J.S. Liu. Effects of chloride ions on bleaching of azo dyes by Co^{2+} /oxone reagent: kinetic analysis. *J. Hazard. Mater.* 190 (2011) 1083–1087.
- [21] Y.R. Wang, W. Chu. Photo-assisted degradation of 2,4,5-trichlorophenoxyacetic acid by Fe(II)-catalyzed activation of Oxone process: The role of UV irradiation, reaction mechanism and mineralization. *Appl. Catal. B Environ.* 123-124 (2012) 151-161.
- [22] G.P. Anipsitakis, D.D. Dionysiou. Degradation of organic contaminants in water with sulfate radicals generated by the conjunction of peroxymonosulfate with cobalt. *Environ. Sci. Technol.* 37 (2003) 4790–4797.
- [23] E.R. Bandala, M.A. Peláez, D.D. Dionysiou, S. Gelover, J. Garcia, D. Macías. Degradation of 2,4-dichlorophenoxyacetic acid (2,4-D) using cobalt-peroxymonosulfate in Fenton-like process. *J. Photoch. Photobio. A* 186 (2007) 357–363.
- [24] Z.Y. Yu, L. Kiwi-Minsker, A. Renken, J. Kiwi. Detoxification of diluted azo-dyes at biocompatible pH with the Oxone/ Co^{2+} reagent in dark and light processes. *J. Mol. Catal. A Chem.* 252 (2006) 113–119.
- [25] United States Environmental Protection Agency. Method 410.4. The determination of chemical oxygen demand by semi-automated colorimetry (1993).
- [26] A.D. Eaton, L.S. Clesceri, E.W. Rice, A.E. Greenberg, M.A.H. Franson. *Standard Methods for the Examination of Water and Wastewater*, 21st ed. (2005) APA-AWWA-WEF.
- [27] ISO 7888:1985. Water quality -- Determination of electrical conductivity.

- [28] ISO 7027:1999. Water quality -- Determination of turbidity.
- [29] V.L. Singleton, J.A. Rossi. Colorimetry of total phenolics with phosphomolybdic phosphotungstic acid reagents. *Am. J. Enol. Vitic.* 16 (1965) 144-158.
- [30] L.C. Ferreira, M.S. Lucas, J. R. Fernandes, P.B. Tavares. Photocatalytic oxidation of Reactive Black 5 with UV-A LEDs. *J. Environ. Chem. Eng.* 4 (2016) 109-114.
- [31] J. Rodríguez-Chueca, L.C. Ferreira, J. R. Fernandes, M.S. Lucas, P.B. Tavares, J.A. Peres. Photocatalytic discolouration of Reactive Black 5 by UV-A LEDs and solar radiation. *J. Environ. Chem. Eng.* 3 (2015) 2948-2956.
- [32] J.R. Bolton, K.G. Bircher, W. Tumas, C.A. Tolman. Figures-of-merit for the technical development and application of advanced oxidation technologies for both electric- and solar-driven systems. *Pure Appl. Chem.* 73 (2001) 627–637.
- [33] J. Sun, X. Li, J. Feng, X. Tian. Oxone/Co²⁺ oxidation as an advanced oxidation process: Comparison with traditional Fenton oxidation for treatment of landfill leachate. *Water Res.* 43 (2009) 4363-4369.
- [34] F.J. Rivas, O. Gimeno, T. Borallho. Aqueous pharmaceutical compounds removal by potassium monopersulfate. Uncatalyzed and catalyzed semicontinuous experiments. *Chem. Eng. J.* 192 (2012) 326-333.
- [35] Y.R. Wang, W. Chu. Degradation of a xanthene dye by Fe(II)-mediated activation of Oxone process. *J. Hazard. Mater.* 186 (2011) 1455-1461.
- [36] K.Ch. Huang, R.A. Couttenye, G.E. Hoag. Kinetics of heat-assisted persulfate oxidation of methyl tert-butyl ether (MTBE). *Chemosphere* 49 (2002) 413–420.

- [37] J. Fernández, P. Maruthamuthu, A. Renken, J. Kiwi. Bleaching and photobleaching of Orange II within seconds by the oxone/ Co^{2+} reagent in Fenton-like processes. *Appl. Catal. B Environ.* 49 (2004) 207-215.
- [38] Y. Zhiyong, L. Kiwi-Minsker, A. Renken, J. Kiwi. Detoxification of diluted azo-dyes at biocompatible pH with the oxone/ Co^{2+} reagent in dark and light processes. *J. Mol. Catal. A Chem.* 252 (2006) 113-119.
- [39] G.P. Anipsitakis, D.D. Dionysiou. Transition metal/UV-based advanced oxidation technologies for water decontamination. *Appl. Catal. B Environ.* 54 (2004) 155-163.
- [40] J.J. Pignatello. Dark and photoassisted iron(3+)-catalyzed degradation of chlorophenoxy herbicides by hydrogen peroxide. *Environ. Sci. Technol.* 26 (1992) 944–951.
- [41] H. Gallard, J. De Laat, B. Legube. Spectrophotometric study of the formation of iron(III)-hydroperoxy complexes in homogeneous aqueous solutions. *Water Res.* 33 (1999) 2929–2936.
- [42] M.M. Ahmed, M. Brienza, V. Goetz, S. Chiron. Solar photo-Fenton using peroxymonosulfate for organic micropollutants removal from domestic wastewater: Comparison with heterogeneous TiO_2 photocatalysis. *Chemosphere* 117 (2014) 256-261.
- [43] F. Ji, C. Li, L. Deng. Performance of CuO/Oxone system: Heterogeneous catalytic oxidation of phenol at ambient conditions. *Chem. Eng. J.* 178 (2011) 239-243.
- [44] J. Madhavan, P. Maruthamuthu, S. Murugesan, S. Anandan. Kinetic studies on visible light-assisted degradation of acid red 88 in presence of metal-ion coupled Oxone reagent. *Appl. Catal. B Environ.* 83 (2008) 8–14.

- [45] M.G. Antoniou, A.A. de la Cruz, D.D. Dionysiou. Degradation of microcystin-LR using sulfate radicals generated through photolysis, thermolysis and e^- transfer mechanisms. *Appl. Catal. B Environ.* 96 (2010) 290-298.
- [46] J.A. Khan, X. He, N.S. Shah, H.M. Khan, E. Hapeshi, D. Fatta-Kassinos, D.D. Dionysiou. Kinetic and mechanism investigation on the photochemical degradation of atrazine with activated H_2O_2 , $S_2O_8^{2-}$ and HSO_5^- . *Chem. Eng. J.* 252 (2014) 393-403.
- [47] J. Sharma, I.M. Mishra, D.D. Dionysiou, V. Kumar. Oxidative removal of Bisphenol A by UV-C/peroxymonosulfate (PMS): Kinetics, influence of co-existing chemicals and degradation pathway. *Chem. Eng. J.* 276 (2015) 193-204.
- [48] S. Khan, X. He, H. Khan, D. Boccelli, D.D. Dionysiou. Efficient degradation of lindane in aqueous solution by iron (II) and/or UV activated peroxymonosulfate. *J. Photochem. Photobiol. A* 316 (2016) 37-43.
- [49] M.S. Lucas, J.A. Peres. Removal of COD from olive mill wastewater by Fenton's reagent: kinetic study. *J. Hazard. Mater.* 168 (2009) 1253-1259.
- [50] J.A. Khan, X. He, H.M. Khan, N.S. Shah, D.D. Dionysiou. Oxidative degradation of atrazine in aqueous solution by UV/ H_2O_2/Fe^{2+} , UV/ $S_2O_8^{2-}/Fe^{2+}$ and UV/ HSO_5^-/Fe^{2+} processes: A comparative study. *Chem. Eng. J.* 218 (2013) 376-383.
- [51] Y. Deng, J.D. Englehardt. Treatment of landfill leachate by the Fenton process. *Water Res.* 40 (2006) 3683-3694.
- [52] A. Rastogi, S.R. Al-Abed, D.D. Dionysiou. Sulfate radical-based ferrous-peroxymonosulfate oxidative system for PCBs degradation in aqueous and sediment systems. *Appl. Catal. B. Environ.* 85 (2009) 171-179.

[53] P. Neta, R.E. Huie, A.B. Ross. Rate constants for reactions of inorganic radicals in aqueous solution. *J. Phys. Chem. Ref. Data* 17 (1988) 1027-1284.

Table captions

Table 1. Winery wastewater physicochemical characteristics.

Table 2. Electrical energy per order (E_{EO}) values of PMS/Co(II) treatments assisted by different UV radiation sources.

Table 3. COD removal values in the PMS/Co(II)/UV-A LED treatment process with different initial COD concentration. Experimental conditions: 2.5 mM PMS; 1 mM Co(II); UV-A LEDs 70 W/m²; pH 6.5; T = 323 K; 180 minutes.

Table 4. Total polyphenols removal through PMS/Mⁿ⁺/UV-A LEDs treatments after 180 minutes at pH 6.5.

Figure captions

Figure 1. COD removal in the optimization of a) pH, b) temperature, c) PMS concentration and d) Co(II) concentration (reaction time 90 minutes).

Figure 2. Influence of different sulphate salts in the removal of COD. Experimental conditions: 2.5 mM PMS; 1 mM M^{n+} ; pH 6.5; T = 323 K; 90 minutes.

Figure 3. Influence of UV source in the PMS/Co(II)/UV treatment process. (▲) UV-A LEDs 70 W/m²; (■) UV-A LEDs 23 W/m²; (●) UV mercury lamp; (◇) No radiation. Experimental conditions: 2.5 mM PMS; 1 mM Co(II); pH 6.5; T = 323 K; 120 minutes. Note: each UV source has different radiation flux.

Figure 4. Influence of transition metals [Co(II) or Fe(II)] in COD and TOC removal: (a) 323 K; (b) ambient temperature (293 K). Experimental conditions: COD = 5000 mg O₂/L; 2.5 mM PMS; 1 mM M^{n+} ; UV-A LEDs 70 W/m²; pH 6.5; 180 minutes.

Figure 5. The effect of different dosing steps on COD removal: one addition of 20/8 mM PMS/Co(II) or six additions of 3.33/1.33 mM PMS/Co(II). Experimental conditions: COD = 5000 mg O₂/L; UV-A LEDs 70 W/m²; pH 6.5; T = 323 K; 180 minutes.

Figure 6. Comparison of SR-AOPs and HR-AOPs on COD and TOC removal at: (a) 323 K; (b) ambient temperature (293 K). Experimental conditions: COD = 5000 mg O₂/L; 2.5 and 20 mM oxidant agent (PMS or H₂O₂); 1 and 8 mM Fe(II); UV-A LEDs 70 W/m²; pH 6.5; 180 minutes.

Figure 7. The effect of temperature on COD and TOC removal by photo-Fenton treatments. Experimental conditions: COD = 5000 mg O₂/L; 2.5 and 20 mM H₂O₂; 1 and 8 mM Fe(II); UV-A LEDs 70 W/m²; pH 3; 180 minutes.

